

## Microtubules in the metaphase-arrested mouse oocyte turn over rapidly

(meiosis/mitosis/microtubule dynamics/photobleaching/spindle)

GARY J. GORBSKY\*<sup>†</sup>, CALVIN SIMERLY<sup>‡</sup>, GERALD SCHATTEN<sup>‡</sup>, AND GARY G. BORISY<sup>‡</sup>

<sup>†</sup>Integrated Microscopy Resource for Biomedical Research and Laboratory of Molecular Biology, University of Wisconsin, Madison, WI 53706; and

<sup>‡</sup>Department of Anatomy and Cell Biology, University of Virginia Health Sciences Center, Charlottesville, VA 22908

Communicated by Neal L. First, May 14, 1990

**ABSTRACT** After ovulation mammalian oocytes arrest in second meiotic metaphase. We asked whether the microtubules that comprise the meiotic spindle of mouse oocytes were stable or were undergoing rapid cycles of assembly and disassembly. Porcine brain tubulin, derivatized with biotin or x-rhodamine [5- (and -6)-carboxy-x-rhodamine], was microinjected into living oocytes. Biotinylated tubulin incorporated into the meiotic spindle to apparent equilibrium within 15 min. To assess quantitatively the rates of disassembly and assembly of the microtubules, small domains within the spindles of oocytes injected with x-rhodamine-tubulin were photobleached and their recovery was analyzed by digital imaging microscopy. Fluorescence recovery in the spindles was rapid and extensive, plateauing to an average of 83% at 4 min. The calculated half-time for turnover of the spindle microtubules was 77 sec. In contrast, fluorescence recovery of the spindle midbodies in telophase oocytes was much more limited, averaging  $\approx 22\%$  at 4 min. These data indicate that most microtubules within the arrested metaphase spindle of the mouse oocyte undergo rapid cycles of assembly and disassembly. Microtubules of the telophase midbody are more stable.

Recent studies of living cells microinjected with fluorescent tubulin (1–4) have eroded the notion that microtubules are static structures. For the bulk of the microtubule array in cultured cells in interphase, estimates of the half-time for disassembly and reassembly range from 5 to 15 min (3–5). Rapid length changes at the ends of microtubules, growth at 3.5–7.2  $\mu\text{m}/\text{min}$  and disassembly at 4.3–18.5  $\mu\text{m}/\text{min}$ , have been directly observed in the thin lamellae of well-spread cells (6–8). Microtubule turnover is yet more rapid in the mitotic metaphase spindles of living mammalian cells and early echinoderm embryos, exhibiting half-times from 15 to 70 sec (1, 2, 9, 10). This rapid assembly and disassembly of microtubules may play an important role in the proper positioning and segregation of the chromosomes.

In contrast to the generally inexorable transit of cells through mitosis, oocytes are often arrested at particular stages of meiosis that are characteristic for each species (11). In mammals such as mice, mature oocytes within the ovary are arrested at meiotic prophase. The oocyte, under the influence of luteinizing hormone, is released from the ovary and undergoes the first meiotic division with the production of the first polar body. The egg then enters another period of stasis in development, arresting at second meiotic metaphase as it moves into the oviduct. The egg may remain arrested in this state for several hours awaiting fertilization and final maturation. Recently it was shown that expression of the *c-mos* protooncogene is the “cytostatic factor” that arrests *Xenopus* oocytes in metaphase of meiosis II (12). The *mos*-encoded protein was found to be proteolyzed upon fertiliza-

tion of *Xenopus* eggs (13). Presumably, destruction of the *mos* protein allows progression through meiosis and initiation of the mitotic cycles of embryonic cleavage. The *mos* protein is also present and required for normal meiotic maturation in mouse oocytes (14).

The alignment of the chromosomes at the metaphase plate is normally a transient event in meiosis and mitosis. The mechanism by which this alignment is stabilized in mature oocytes, often for many hours, is unknown. Conceptually, once initially arrived at the metaphase plate, chromosomes might be constrained from dispersing in at least two ways. The first way would be to prohibit further motion of the chromosomes through stabilization of the spindle microtubules. The second way would be to hold the chromosomes to the metaphase plate dynamically through a balance of equal and oppositely directed, active forces. One manner in which to distinguish these possibilities is to determine whether the oocyte has static or rapidly cycling microtubules.

The stability of the arrested meiotic spindle has been studied in eggs of marine invertebrates. In the marine annelid *Chaetopterus*, one meiotic pole is attached to the cell cortex. Perturbations such as cooling (15) or the application of hydrostatic pressure (16) cause spindle birefringence to diminish through the depolymerization of microtubules. If the perturbations are induced gradually, the chromosomes are transported to the cortex as the birefringence disappears. When the perturbations are removed, the chromosomes return to their metaphase location accompanying the reappearance of the spindle birefringence. Inoue and Ritter (15) interpreted such experiments to indicate that the spindle fibers in the arrested metaphase oocyte were in “dynamic equilibrium” between a pool of assembled polymer and unassembled monomer; cold or pressure caused a shift in equilibrium toward the monomer.

As in other meiotic or mitotic cells, the metaphase alignment of the chromosomes in mouse oocytes is dependent upon intact microtubules since microtubule-disrupting drugs will abolish it (17). However, microtubules within the meiotic spindle of the mouse oocyte might be expected to exhibit dynamics distinct from those of mitotic cells of embryos and cultured mammalian cells where metaphase duration is short and where microtubules cycle rapidly. Mouse oocytes have other unusual features. The spindles contain a large proportion of acetylated tubulin (18, 19), a posttranslational modification of the  $\alpha$ -tubulin molecule that is found within microtubules that are often, though not always, more stable than the general population within a cell (20). Moreover, unlike other animal cells, the mouse oocyte as well as the early cleavage stage embryo contain no centrioles (21). We set out to directly measure, with minimal perturbation, microtubule turnover in the arrested meiotic spindle of the mouse oocyte. Our measurements of incorporation of microinjected tubulin

The publication costs of this article were defrayed in part by page charge payment. This article must therefore be hereby marked “advertisement” in accordance with 18 U.S.C. §1734 solely to indicate this fact.

<sup>†</sup>To whom reprint requests should be addressed at: Box 439, Health Sciences Center, University of Virginia, Charlottesville, VA 22908.

and the rate of fluorescence recovery after photobleaching indicate that turnover of the spindle microtubules within the mouse oocyte is rapid.

### MATERIALS AND METHODS

**Incorporation of Biotinylated Tubulin.** Biotinylated (22), polymerization-competent tubulin (biotin-tubulin) (10 mg/ml) from porcine brain was microinjected into zona-intact, unfertilized oocytes according to the methods of Uehara and Yanagimachi (23) and Thadani (24). Injected oocytes were maintained in M-2 culture medium (25) at 37°C for varying time spans before processing for indirect immunofluorescence as described (17). Briefly, oocytes were incubated for 30 sec in pH 2.5 M-2 culture medium to remove the zona pellucidae. The denuded oocytes were permeabilized in a microtubule-stabilizing buffer composed of 25% (vol/vol) glycerol, 50 mM KCl, 0.5 mM MgCl<sub>2</sub>, 0.1 mM EGTA, 1 mM 2-mercaptoethanol, and 50 mM imidazole hydrochloride at pH 6.8 with 1% Triton X-100. After affixing extracted oocytes onto polylysine-coated coverslips, cells were fixed in methanol (-10°C) for 5 min. Injected biotin-tubulin was detected with fluorescein-streptavidin (1:25 dilution; Jackson ImmunoResearch) applied to coverslips for 40 min. To permit a comparison of newly incorporated biotin-tubulin versus the total microtubule network, all microtubules in the mouse cytoskeletons were labeled using an affinity-purified rabbit anti-tubulin antibody (50 µg/ml) applied for 40 min and imaged with rhodamine-conjugated anti-rabbit IgG secondary antibody (40 min; 1:20 dilution; Cappel Laboratories).

DNA was fluorescently labeled by addition of 2.5 µg of 4',6-diamidino-2-phenylindole per ml (Sigma) to the final rinse in phosphate-buffered saline. All images were photographed on Kodak Tri-X film with a Zeiss Axiophot epifluorescent microscope equipped with a ×100 plan-Neofluar (1.3 numerical aperture) objective and differential interference contrast optics. Fluorescent intensities of newly incorporated versus total microtubules were qualitatively compared on negatives and prints exposed under identical times.

**Photobleaching and Recovery.** Polymerization-competent porcine brain tubulin, derivatized with x-rhodamine [5- (and -6)-carboxy-x-rhodamine], was prepared as described (8) and microinjected into mouse oocytes. Photobleaching of metaphase spindles of oocytes was performed at 34–36°C in M-2 culture medium prepared without phenol red using the instrumentation and protocols outlined previously (26). For focusing and orientation of the spindles, short (0.1 sec) exposures with attenuated mercury arc illumination were captured with a silicon intensified target video camera (model 66; Dage-MTI, Wabash, MI) coupled to an image processor (model 9200; Quantex, Sunnyvale, CA). For quantitative analysis, images of living oocytes were captured with a cooled charge-coupled device camera (model 200; Photometrics, Tucson, AZ) and processed as described (9). Measurements were normalized as follows to account for variation in the amount of tubulin injected in each oocyte: intensity = (fluorescent intensity in the bleached zone – baseline fluorescent intensity)/(fluorescent intensity of the prebleach image – baseline fluorescent intensity). For each cell a baseline position was fixed just beyond the outer edge of the

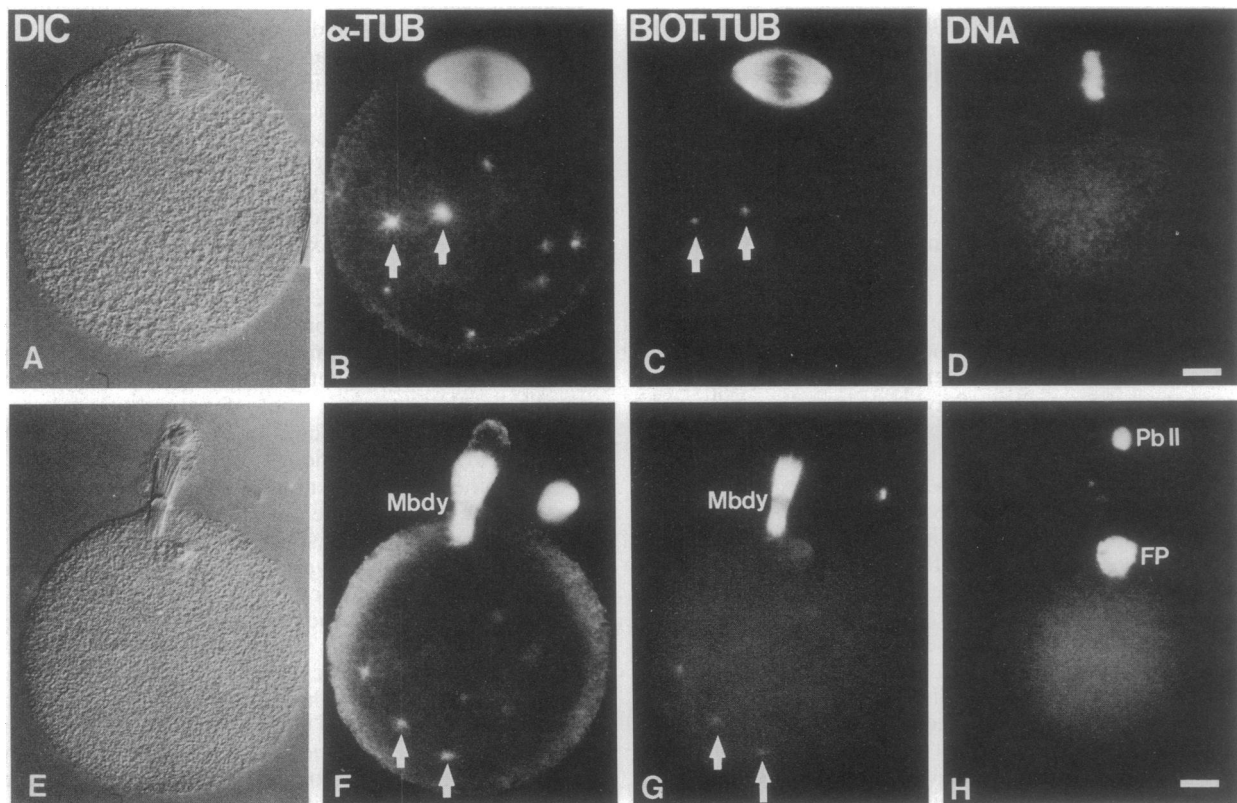


FIG. 1. Incorporation of microinjected biotin-tubulin into mouse meiotic spindles, midbodies, and cytoplasmic microtubules. (A–D) A metaphase-arrested unfertilized oocyte processed 48 min after microinjection with biotin-tubulin. Spindle and cytoplasmic microtubules incorporate biotin-tubulin (C) though incorporation into the cytastral microtubules is primarily detected at the centrosomes (arrows, B and C). (E–H) Biotin-tubulin incorporation in microinjected oocyte that was subsequently activated to proceed to telophase. A meiotic midbody is produced after activation (F, Mbdy) as the female pronucleus (FP) and second polar body nucleus form (H, PbII). The microtubules of the midbody (G, Mbdy) and cytasters (arrows, F and G) contain biotin-tubulin. DIC, differential interference contrast (A and E);  $\alpha$ -TUB, affinity-purified rabbit anti-tubulin antibody (B and F); BIOT. TUB, biotin-tubulin (C and G); DNA, 4',6-diamidino-2-phenylindole staining (D and H). (Bar = 10 µm.)

half-spindle that was not photobleached. The baseline intensity was measured at that position for each image of a cell in a photobleaching series. To correct for fading of fluorescence during image taking, the values obtained above were multiplied by the ratio of the baseline fluorescence intensity in the prebleach image to the baseline intensity at each time  $t$ . Photobleaching was conducted on a total of 15 spindles, of which 8 were of sufficient alignment to use for quantitative analysis. Data were fit to the perturbation-relaxation equation  $F_t = F_i + (F_f - F_i)(1 - e^{-kt})$ , where  $F_t$  is the fluorescence intensity at any time  $t$ ,  $F_i$  is the fluorescence intensity just after photobleaching, and  $F_f$  is the final intensity at time infinity (27). We estimated  $F_f$  from the mean of the final fluorescence recovery measurement of the four spindles observed over the longest time period ( $\approx 4$  min). The fluorescence recovery half-time for the spindle data was evaluated by plotting the early time points (20–120 sec) to the linear transformation of the perturbation-relaxation equation  $\ln(F_t - F_i) = \ln(F_f - F_i) - kt$  (28). The slope of the best-fit line gave the coefficient  $k$ , and the half-time for fluorescence recovery was then calculated from the formula  $t_{1/2} = \ln 2/k$ . Midbodies were produced by parthenogenetically activating oocytes with 7% ethanol (29) and incubating for 30 min at 37°C. Four midbodies were photobleached and analyzed for comparison of their microtubule dynamics with that of the arrested metaphase spindle.

## RESULTS

To evaluate the stability or lability of the microtubules, we microinjected biotin-tubulin into metaphase-arrested mouse oocytes and assessed incorporation into the spindle (Fig. 1). Our earliest observations indicated that the injected tubulin appeared to equilibrate into the oocyte microtubules within 15 min after microinjection.

To determine more precisely the extent and rate of microtubule turnover, we photobleached bars across the fluorescent spindles in cells injected with x-rhodamine-tubulin and recorded the recovery of fluorescence by digital imaging microscopy of the living oocyte. We found that substantial recovery took place rapidly (Fig. 2). Fluorescence in the bleached zones recovered to an average extent of  $83\% \pm 15\%$  (mean  $\pm$  SD) of the original bleach. To calculate the half-time for recovery we fit the data from the incorporation phase of recovery ( $< 120$  sec) to a linear form of the perturbation-relaxation equation (Fig. 3). The slope of the least-squares fit gave a fluorescence recovery half-time of 77 sec with a 95% confidence interval of 57–117 sec. To ensure that our protocol could in fact detect a persistent bleached zone indicating stable microtubules, we photobleached meiotic midbodies obtained after artificial activation of injected oocytes. Microtubules of mitotic midbodies exhibit extraordinary stability to depolymerization by microtubule inhibitors such as nocodazole (30). Thus, as expected, microtubules of the oocyte midbody exhibited limited fluorescence recovery after photobleaching, averaging  $22\% \pm 21\%$  (mean  $\pm$  SD) (data not shown). The variability noted may be due to the precise phase of the cell cycle at which the experiments were performed. For example, midbodies of late anaphase-early telophase oocytes may exhibit greater turnover than those further progressed into interphase.

Given the recent report of a poleward flux in metaphase mammalian cells (31), we wondered whether recovery in the metaphase oocyte spindles could have resulted from rapid poleward movement. We measured the location of the bleached zone with respect to the mitotic pole. Because recovery occurred swiftly, in many of the images from the later time points, a position for the bleached zone could be assigned only within a margin of error of  $\pm 0.5 \mu\text{m}$ . Nonetheless, the data indicated, at most, a slow poleward movement of the bleached zone at  $0.3 \pm 0.2 \mu\text{m}/\text{min}$ . This finding

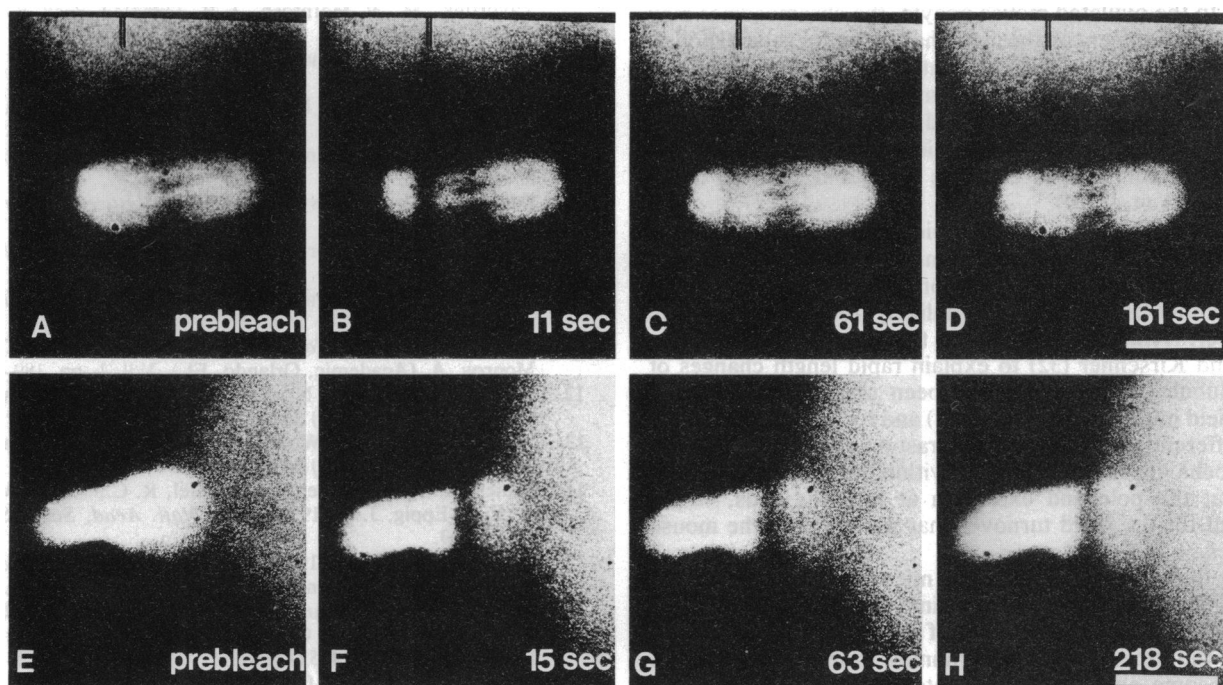


FIG. 2. Fluorescent recovery after photobleaching occurs rapidly in unfertilized mouse oocytes arrested in metaphase of second meiosis but slowly in meiotic midbodies. x-Rhodamine-tubulin microinjected into metaphase-arrested oocytes incorporates into spindle microtubules as detected by live imaging with a cooled charge-coupled device (A, prebleach). Following laser photobleaching of a cylindrical bar across the fluorescent spindle (B), a progression of images after irradiation shows that fluorescent recovery is rapid in the bleached zone (C and D). A prebleach image of a meiotic midbody is shown in E. Following laser photobleaching of a cylindrical bar across the midbody (F), subsequent images (G and H) demonstrate that fluorescent recovery is slow. Times in sec after photobleaching are indicated in the lower right of frames B–D and F–H. (Bar =  $10 \mu\text{m}$ .)

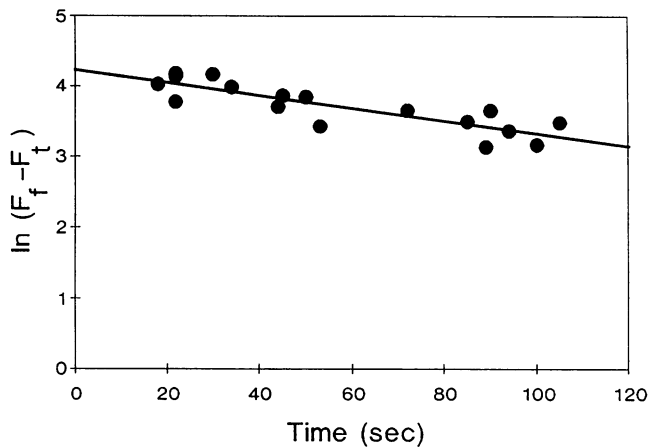


FIG. 3. Incorporation phase of fluorescence recovery analyzed according to the linear transformation of the perturbation-relaxation function. Data were taken from eight spindles photobleached at time 0 and imaged on average three times. From the slope of the line, the coefficient  $k = 0.0090$  generated the half-time for recovery of 77 sec. The 95% confidence interval, 57–117 sec, was calculated from the estimated standard error of the slope = 0.00145.

is similar to the results in cultured mammalian cells (9, 31) but is too slow to account for the bulk of fluorescence recovery measured in the arrested metaphase spindles of mouse meiotic oocytes.

### DISCUSSION

The swift incorporation of biotin-tubulin and rapid recovery of fluorescence after photobleaching observed in the mouse oocyte suggest that the bulk of meiotic spindle microtubules are rapidly turning over. This finding is in accord with the ideas of Inoue and Ritter (15), who suggested that even within spindles arrested in meiotic metaphase, turnover would continue. In the ovulated mouse oocyte, the chromosomes may hold their alignment on the metaphase plate for several hours. Nonetheless, our evidence indicates that most of the microtubules of metaphase-arrested mouse oocytes are highly dynamic, exhibiting assembly and disassembly rates comparable to those found among microtubules in the mitotic spindles of echinoderm embryos (1, 2) and cultured mammalian cells (4, 9, 10).

The mechanism behind this rapid cycling of spindle microtubules remains uncertain. Our limited evidence suggests that a flux of subunits—i.e., addition at the kinetochore and disassembly at the pole—is unlikely to account for the turnover. Dynamic instability is a theory proposed by Mitchison and Kirschner (32) to explain rapid length changes of microtubules *in vitro* and has been observed directly by dark-field microscopy *in vitro* (33) and by fluorescence (7, 8) and differential interference contrast microscopy *in vivo* (6). Such behavior of microtubules within the living cell, nucleation at the pole and extension at the plus ends, would account for the rapid turnover that we detect in the mouse oocytes.

One difficulty in interpreting microinjection and photobleaching experiments in the spindles of living cells is the presence of different categories of microtubules—e.g., those within the kinetochore fiber running from the pole to the chromosome and those nonkinetochore microtubules that extend from the pole into the cytoplasm. The kinetochore fiber is itself heterogeneous, consisting of microtubules that run all the way from the pole to the kinetochore, those with one free end and those with both ends free in the fiber (34). Within the arrested mouse egg we have no good estimate of the proportion of microtubules of the various classes. Thus our observations that turnover is rapid reflect the behavior of

the bulk population of microtubules. Analysis of subpopulations must await the application of methods for study at higher resolution.

In the ovulated mouse oocyte, the chromosomes may hold their alignment on the metaphase plate for several hours. What function might the rapid cycling of microtubules perform in the arrested mammalian oocyte? One possibility is that the rapid dynamics in metaphase are required so the cell can proceed immediately into anaphase upon fertilization. Another speculation is that microtubule turnover is necessary to maintain the metaphase configuration. Rieder *et al.* (35) have suggested that ejection forces, produced by the continuous nucleation and growth of microtubules from the poles, are involved in driving chromosomes to the metaphase alignment. Perhaps such forces are essential to prevent the chromosomes from drifting off the metaphase plate. Although current information is yet insufficient to settle this issue, our results suggest that rapid microtubule dynamics may be important in the proper segregation of chromosomes in meiosis.

We thank Randy Prather, John Peloquin, Paul Sammak, Vicki Centonze, and Steven Limbach for their invaluable assistance in carrying out these experiments. The support of this work by research grants from the National Institutes of Health to G.G.B. and G.S. is gratefully acknowledged. The Integrated Microscopy Resource for Biomedical Research is funded as a National Institutes of Health Biomedical Research Technology Resource. G.J.G. was supported in part by the University of Virginia Cancer Center and by Grant IN-149E from the American Cancer Society.

1. Hamaguchi, Y., Toriyama, M., Sakai, H. & Hiramoto, Y. (1987) *Cell Struct. Funct.* **12**, 43–52.
2. Salmon, E. D., Leslie, R. J., Saxton, W. M., Karow, M. L. & McIntosh, J. R. (1984) *J. Cell Biol.* **99**, 2165–2174.
3. Sammak, P. J., Gorbsky, G. J. & Borisy, G. G. (1987) *J. Cell Biol.* **104**, 395–405.
4. Saxton, W. M., Stemple, D. L., Leslie, R. J., Salmon, E. D., Zavortink, M. & McIntosh, J. R. (1984) *J. Cell Biol.* **99**, 2175–2186.
5. Schulze, E. & Kirschner, M. (1986) *J. Cell Biol.* **102**, 1020–1031.
6. Cassimeris, L., Pryer, N. K. & Salmon, E. D. (1988) *J. Cell Biol.* **107**, 2223–2231.
7. Schulze, E. & Kirschner, M. (1988) *Nature (London)* **334**, 356–359.
8. Sammak, P. J. & Borisy, G. G. (1988) *Nature (London)* **332**, 724–726.
9. Gorbsky, G. J. & Borisy, G. G. (1989) *J. Cell Biol.* **109**, 653–662.
10. Wadsworth, P. & Salmon, E. D. (1986) *J. Cell Biol.* **102**, 1032–1038.
11. Masui, Y. (1985) in *Biology of Fertilization*, eds. Metz, C. B. & Monroy, A. (Academic, Orlando, FL), Vol. 1, pp. 189–219.
12. Sagata, N., Watanabe, N., Vande Woude, G. F. & Ikawa, Y. (1989) *Nature (London)* **342**, 512–518.
13. Watanabe, N., Vande Woude, G. F., Ikawa, Y. & Sagata, N. (1989) *Nature (London)* **342**, 505–511.
14. Paules, R. S., Buccione, R., Moschel, R. C., Vande Woude, G. F. & Eppig, J. J. (1989) *Proc. Natl. Acad. Sci. USA* **86**, 5395–5399.
15. Inoue, S. & Ritter, H. (1975) in *Molecules and Cell Movement*, eds. Inoue, S. & Stephens, R. E. (Raven, New York), pp. 3–30.
16. Salmon, E. D. (1975) *Ann. N.Y. Acad. Sci.* **253**, 383–406.
17. Schatten, G., Simerly, C. & Schatten, H. (1985) *Proc. Natl. Acad. Sci. USA* **82**, 4152–4156.
18. Schatten, G., Simerly, C., Asai, D., Szoke, E., Cooke, P. & Schatten, H. (1988) *Dev. Biol.* **130**, 74–86.
19. dePennart, H., Houliston, E. & Maro, B. (1988) *Biol. Cell* **64**, 375–378.
20. Webster, D. R. & Borisy, G. G. (1989) *J. Cell Sci.* **92**, 57–65.
21. Szollosi, D., Calarco, P. & Donohue, R. P. (1972) *J. Cell Sci.* **11**, 521–541.
22. Mitchison, T. J. & Kirschner, M. (1985) *J. Cell Biol.* **101**, 755–765.

23. Uehara, T. & Yanagimachi, R. (1977) *Biol. Reprod.* **16**, 315–321.
24. Thadani, V. M. (1980) *J. Exp. Zool.* **12**, 435–453.
25. Fulton, B. P. & Whittingham, D. G. (1978) *Nature (London)* **273**, 149–151.
26. Gorbsky, G. J., Sammak, P. J. & Borisy, G. G. (1987) *J. Cell Biol.* **104**, 9–18.
27. Jacobson, K., Derko, Z., Wu, E.-S., Hou, Y. & Poste, G. (1976) *J. Supramol. Struct.* **5**, 565–576.
28. Wadsworth, P. & Salmon, E. D. (1985) *Ann. N.Y. Acad. Sci.* **466**, 580–592.
29. Cuthbertson, K. S. R. (1983) *J. Exp. Zool.* **226**, 311–314.
30. DeBrabander, M., Geuens, G., Nuydens, R., Willebrords, R., Aerts, F. & DeMey, J. (1986) *Int. Rev. Cytol.* **101**, 215–275.
31. Mitchison, T. J. (1989) *J. Cell Biol.* **109**, 637–652.
32. Mitchison, T. & Kirschner, M. (1984) *Nature (London)* **312**, 237–242.
33. Horio, T. & Hotani, H. (1986) *Nature (London)* **321**, 605–607.
34. Rieder, C. L. (1981) *Chromosoma* **84**, 145–158.
35. Rieder, C. L., Davison, E. A., Jensen, L. C. W., Cassimeris, L. & Salmon, E. D. (1986) *J. Cell Biol.* **103**, 581–591.